Article

Extension of the Set of Raw Sludges used in Industrial Anaerobic Digestion Reactors Implementable in Control Schemes Using an On-line Model Parameter Identification Strategy

Luis G. Cortés [1,†,‡], Julio Barbancho [1], María A. De la Rubia [2],Diego F. Larios [1], Jose D. Marín [2], A.F. Mohedano [2], Christian Portilla [3]

[1] Department of Electronic Technology, Polytechnic School, University of Seville; luicoroca@alum.us.es
[2] Chemical Engineering Department, Universidad Autonoma de Madrid, Campus de Cantoblanco, 28049, Madrid, Spain; angeles.delarubia@uam.es
[3] Facultad de Minas, Universidad Nacional de Colombia, Robledo, 050034, Medellín, Antioquia; crportil@unal.edu.co
* Correspondence: luicoroca@alum.us.es; Tel.: +34 656957248 (Spain)
† Escuela Politécnica Superior de la Universidad de Sevilla, Calle Virgen de África, 7, 41011 Seville, Spain
‡ These authors contributed equally to this work.

Abstract: This work presents a methodology that seeks to be a new standard in modeling identification in anaerobic digestion reactors. Because it is not possible to measure all variables with reliable and cost-efficient real-time methods, a specific structure composed of an asymptotic observer for the concentration of state variables; acidogenic and methanogenic bacterias, unlock the use of new types of raw sludges for industrial control and monitoring purposes. New yield parameters were included in the reduced anaerobic digestion model (ADM2) used as the core, precisely two terms in total alkalinity, to bring about the modeling of additional organic materials at inlet containing proteins or amino acids. The fermentation of these substances introduces ammonium, providing variations in the amount of alkalinity available inside the reaction. The new model is used to solve an optimization problem that calculates the parameters that best fit the dynamics of state variables with the same information taken on the experimental data. The adjustment process started with the genetic algorithm; however, to improve the performance, a novel method is proposed called step-ahead. Together, including the design of an asymptotic observer, numerical simulations demonstrate the strengths of the structure, which constitutes a significant step in paving the way further to implement feasible, cost-effective control and monitoring systems in the industry.

Keywords: asymptotically observer; homogeneous reaction systems; anaerobic digestion; volatile fatty acids

1. Introduction

Anaerobic digestion (AD) is a complex biological process where a consortium of anaerobic microorganisms, in the absence of oxygen, break down a biodegradable fraction of biomass into biogas and digestate [1]. The organic matter takes place inside a sealed vessel (reactor). Compared to other common alternatives, such as aerobic treatment systems, the AD process return little sludges, have a positive overall energy balance, and also has an enormous potential to reduce challenging and concentrated substrates such as animal wastes, wastewater, by-products from industrial plants, and food wastes to name the most important ones [2]. However, despite these benefits, the technology is not yet used extensively in large-scale industries. The reasons behind this are; that the control systems, trying to balance the operational requirements inside the reactor, failed because the reaction becomes easily unstable due to slight sensitive variations in biological rates [3]. The arguments mentioned above support why full-scale reactors are mainly still operated manually [4], because its efficiency depends mainly on the expertise of based-knowledge operators and

 doi:10.20944/preprints202208.0395.v1

the process circumstances, becoming a challenge if the purpose is to develop a technology that operates massively. However, these obstacles explain why such research area has been active by scientists during the last years, allowing to improve the performance of reactors and maintain them over stable operational conditions [5,6].

Typically those systems inherently act with non-linear nature. In addition, essential singularities, such as high sensitiveness to uncontrollable inputs and perturbations, and the drawbacks caused by the restricted access to online measurements (due to the lack of cost-efficient and reliable sensors), originate mathematical models with limited approximations. The effort begins with setting a reliable architecture based on non-linear monitoring and control schemes to overcome these inconveniences. While there exists a varied number of alternatives, based on mathematical modeling found in the literature that demonstrates good efficiency, generalization and partial knowledge of the phenomena are the main challenges to solve, especially if the main goal is to develop scalable software as the basis of implementations on the large-scale industry.

The phenomenology is frequently poorly comprehended because the anaerobic digestion processes are related to the existence of microorganisms. Then, replicating mathematically the same operating conditions are not possible regularly due to the uncertainty and variation in yield parameters because of changes in metabolism. This paper aims to contribute with a novel software beyond traditional methods, where performance depends on measured data and new software sensors strategies that capture the reality with high reliability. To perform a long-term plan to achieve feasible control schemes for industrial purposes, the first step is to ensure the existence of a measurable layer that provides continued data to the mathematical model. Although these observer strategies have been widely used on different types of microorganisms inside a reactor, there are still obstacles in trying to define a method that guarantees full knowledge of the data inside a reaction [7].

A desirable alternative used in literature, the asymptotic observers, estimate the state variables that cannot be measured directly over systems. Depending on the information available, the design of the observer mainly depends on two conditions; the information available regarding the reaction kinetics and the yield parameters. This paper uses a mathematical model AM2 with additional terms to consider a wide range of organic matter modeled at the inlet. With the use of this model, it is still not possible to obtain information on the state variables concentrations of acidogenic X_1 and methanogenic X_2 using feasible online sensors. Additionally, there is no complete knowledge of the process kinetics. Therefore, based on the preliminary information, this paper focuses on developing an asymptotic observer conditioned by the following characteristics; the state variables X_1 and X_2 are unknown, and the yield parameters are known and calculated using a parameter identifications procedure based on optimization. The main challenge resides in using real data from an industrial process that evaluates the proposed methodology in a wide range of possibilities [8,9].

In order to start demonstrating well-performance indicators in the online model parameter identification strategy, the following sections have been proposed as follows. In section 2, a reduced model ADM2 with additional terms for control purposes is presented. Then, in section 3, experimental results are performed in an anaerobic digestion reactor to use as a basis for setting the experimental conditions to test the methods proposed. In section 4, the parameter identification algorithm is presented where an optimization problem is solved to find the values that better fit the dynamics of the mathematical model and the experimental data. Section 5 proposes an asymptotic observer with the condition that the information from reaction rates is unknown. This algorithm aims to estimate the concentrations of acidogenic and methanogenic microorganisms. Finally, on the conclusions, some remarks are discussed coming from the evaluation of performance from the strategy proposed.

Preprints (www.preprints.org) | NOT PEER-REVIEWED | Posted: 23 August 2022 doi:10.20944/preprints202208.0395.v1

2. The anaerobic Digestion Mass-Balance Model

Among the alternatives encountered in the literature that propose reduced mathematical models aiming to deploy control and monitoring systems, the ADM2 mathematical model is considered the best practical option available; it becomes the cornerstone between the anaerobic digestion process on site and feasible controller schemes. The lack of phenomenological knowledge, the high level of difficulties over the process, its nonlinearities, and the lack of reliable sensors support why almost all of the mathematical models found in the literature work as coarse approximations [2]. Therefore is the reason why it is necessary to find reduced models that have the potential to evade the absence of phenomenological knowledge. The alternative proposed in this paper based on mass-balance specifications beats this difficulties positioning the lack of information over specific terms called reaction rates.

The ADM2 reduced model proposed considers biological phase reactions, dividing the consortium into two homogeneous groups; acidogens and methanogens that represent the destabilization phenomenon [2]. To incorporate a broader spectrum of usable organic matter, the influence of ammonium on alkalinity is considered because it is usual to find these compounds when fermentation and microbial growth metabolism occur. Thus, two yield parameters were added to represent this effect; $K_{Z,1}$ and $K_{Z,2}$ respectively. Based on the considerations made by Kil et al. [5], the term $(K_{Z,1}\rho_1 - K_{Z,2}\rho_2)$ is added to the dynamic of the total alkalinity equation proposed by Bernard et al. [2]. The content of waste sludges influences the new yield parameters. In conclusion, the new equation system that represents the anaerobic digestion process is shown in the following equations.

$$\frac{dX_1}{dt} = X_1(\mu_1 - \alpha D), \tag{1}$$

$$\frac{dX_2}{dt} = X_2(\mu_2 - \alpha D), \tag{2}$$

$$\frac{dS_1}{dt} = D(S_{1_{in}} - S_1) - \psi_1\left(\frac{S_1}{K_{S1} + S_1}\right), \tag{3}$$

$$\frac{dS_2}{dt} = D(S_{2_{in}} - S_2) + k_{s_2,1}\psi_1\left(\frac{S_1}{K_{S1} + S_1}\right) - \psi_2\left(\frac{S_2}{K_{S2} + S_2}\right), \tag{4}$$

$$\frac{dZ}{dt} = D(Z_{in} - Z) + k_{Z,1}\psi_1\left(\frac{S_1}{K_{S1} + S_1}\right) + k_{Z,2}\psi_2\left(\frac{S_2}{K_{S2} + S_2}\right), \tag{5}$$

$$\frac{dC}{dt} = D(C_{in} - C) - q_C + k_4\mu_1 X_1 + k_5\mu_2 X_2, \tag{6}$$

with:

$$q_C = k_L a[C + S_2 - Z - K_H P_C] \tag{7}$$

where P_C and Φ comes from the equations described in Bernard et al. [2].

$$P_C = \frac{\Phi - \sqrt{\Phi^2 - 4K_H P_T(C + S_2 - Z)}}{2K_H} \tag{8}$$

with:

$$\Phi = C + S_2 - Z + K_H P_T + \frac{k_6}{k_L a}\mu_2 X_2 \tag{9}$$

From the equations above, X_1 represents the concentration of acidogenic bacterias, X_2 the concentration of methanogenic archaeas, S_1 the concentration of organic substrate, S_2 the concentration of VFA, Z the total alkalinity, and C the concentration of inorganic carbon. The subscript "in" indicates the influent flow of the correspondent concentrations S_1, S_2, C and Z. D is the dilution rate. The yield coefficients k_1, k_2, k_3, k_4, k_5 and k_6 mean the yield

Preprints (www.preprints.org) | NOT PEER-REVIEWED | Posted: 23 August 2022 doi:10.20944/preprints202208.0395.v1

for COD degradation, the yield for VFA production, the yield for VFA consumption, the yield for CO_2 production, the yield for CO_2 production, and the yield for CH_4 production respectively. Originally, the ADM2 model considers that the reaction rate processes do not affect the total alkalinity; nevertheless, the amino acids and proteins usually are presented on the organic matter. Thus, we decided to incorporate this effect to extend the types of raw sludges that the mathematical model can use. In order to keep a simple mathematical description, we introduce the ammonium contribution to the alkalinity mass-balance proposed by Kil et al. [3,5]. The following Monod-type representations characterize the reaction rates $_1$ and $_2$:

$$\rho_1 = \psi_1 \frac{S_1}{K_{S_1} + S_1} \tag{10}$$

and.

$$\rho_1 = \psi_1 \frac{S_1}{K_{S_1} + S_1}. \tag{11}$$

Where ψ_1, ψ_2, K_{S1}, and K_{S2} describe the maximum rate of acidogenic degradation, the maximum rates of methanogenic degradation, the half-saturation constant associated with substrate S_1, and the half-saturation constant associated with the substrate S_2 respectively. Monod-type kinetics describes the growth of acidogenic bacteria ψ_1 (S_1) and methanogenic archaea ψ_2 (S_2), because, in the fermentation process, the biomass does not register possible VFA accumulation and consequently inhibition. Finally, the methane flow rate produced q_M is proportional to the reaction rate of methanogenesis, as shown in the following equation:

$$q_M = k_{CH_4} \psi_2 \left(\frac{S_2}{K_{S2} + S_2} \right) \tag{12}$$

3. Experimental results and characteristics of the reactor

The data set in this paper were collected from a CSTR pilot plant (150 L) operated at 55 ± 2 ºC (thermophilic range). The experiment took place in a sewage treatment plant in Guadalete (Jerez de la Frontera, Spain). The system operates with diary inlet flow with primary and secondary combined waste sludges. Figure 1 shows the diagram of the structure. The temperature on the jacket is regulated via an internal coil (*Heat unit*) using a PID controller linked by a *Temperature sensor*. The *Influent* receive the raw sludges before water is added on the *Dilution unit*. After that, the *Pump* feeds a dilution rate continuously to the reactor. The liquid-flow speed is measured by an electromagnetic sensor (*Flow liquid meter*). The off-line measurements on the *Effluent*, at the bottom of the reactor, are tested periodically in the laboratory using different procedures and protocols. Finally, the biogas on the reaction is tested by a *Gas analyzer* that quantifies the volume of CH_4 produced. The *Flow gas meter* measures the gas rate produced.

The study was conducted to test the effect of step changes in the solid retention time (SRT) during 338 days. The measurements were obtained using two different sources. The values of treatment efficiency indicators (the amount of COD and VFA reduced at effluent from inlet) and the total alkalinity are measured from sensors measuring the production rate of biogas online and from laboratory protocols and procedures. The experiment starts with a portion of raw sludge at thermophilic temperature. SRT starts in 75 days; it gradually decreases from 40 days followed by 27 days, 20 days, and 15 days (see the details on Table 1). However, for modeling purposes, only a specific range of data was used to discard unstable scenarios, which are unfavorable for modeling purposes due to deviations related to the nature of reactions. The range periods discarded were; the latency period (a dormancy of microorganisms) at the beginning and the latest one due to the presence of high nonlinear (at the end of the experiment when the reactor operates closer to boundaries)

Preprints (www.preprints.org) | NOT PEER-REVIEWED | Posted: 23 August 2022 doi:10.20944/preprints202208.0395.v1

[10]. Therefore, the data selected started on SRT at 40 days (day 46 of the experiment) and moved forward until the end of the stage SRT 20 days (day 253 of the experiment). Finally, 207 days were selected, aiming to work with standard patterns of microorganisms as much as possible.

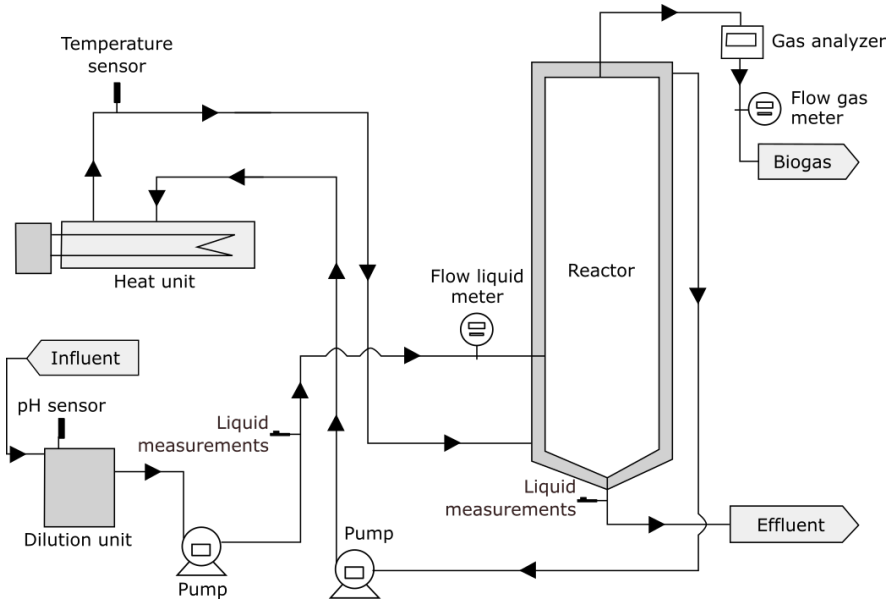

Figure 1. Schematic diagram of the anaerobic digester process in a reactor.

The data selected start at SRT in 40 days, the organic loading rate (OLR) equivalent was 0.8 $KgVS/m^3day$ (or 1.5 $KgCOD/\ m^3\ day$). This value remained constant until the steady state was reached (when the measurements of VS and COD removals and the production rate of CH_4 are the means of the last 15 days' measurements. From the data selected, the first change in the value of SRT occurred on the day 40, where the value of SRT switched to 27 days. At this new stage, the system operates from day 40 until the day 124. Finally, on the day 125, the SRT value decreases to 20 days. This stage took place on the day 124. This value remained constant until the end of the experiment, the day 208.

Table 1. OLR stages during the 338 days experiment.

SRT	Days	
	Start	End
75	1	45
40	46	85
27	86	170
20	171	253
15	254	323

As seen in experimental results, only in specific scenarios does the value of pH decrease beyond 7.3. At this moment, a small amount of sodium carbonate was added at a concentration of 2N to keep the value of pH over a desirable (feasible) operational range. The main attributes of the organic material used are shown in Table 2.

On Figure 2 the level of COD_{in} keeps around 60 g/L with variations in $\pm$ 40 g/L. Only in exceptional cases some values of COD_{in} remain scattered from the mean value. Otherwise, when the VFA_{in} operates at SRT 40 days, the mean value remains closely to 22 g/L with no significant variations. When the reactor operates at SRT values of 27 days and 20 days, there was an upward tendency. On the effluent, Figure 3 shown the values of COD and VFA. The value of COD (see Figure 3a) remained constant during SRT at 40; all values are centred around 18 g/L. After that, in the subsequent stages, at SRT values from 27 to

Preprints (www.preprints.org) | NOT PEER-REVIEWED | Posted: 23 August 2022 doi:10.20944/preprints202208.0395.v1

20, the amount of COD shows a growing irregular tendency. The degree of dispersion is much larger than in the previous period. On the other hand, the values of VFA vary widely, except on SRT at 40 days (see Figure 3b). Only on the stage SRT 40 days the values remain constant around 3 g/L.

Table 2. Main characteristics of the raw sludge.

Parameter	Mean value	Minimal value	Maximum value
COD (kg/m^3)	64	42	74
pH	6.2	5.8	6.4
Sólidos totales (kg/m^3)	55	38	68
Sólidos volátiles (kg/m^3)	68	27	51

Figure 4 shown the consequences of the microbial dynamism derived from the current state of the reactor (see Figures 2 and 3). The volume of CH_4 shown in Figure 4b has a specific behavior at each stage. After surpassing the latency stage, specifically, when the operation of the system changes to SRT 40, the dynamics of bacteria showed a slow linear progression in the volume of CH_4 produced, reaching a maximum of 40 L/day.

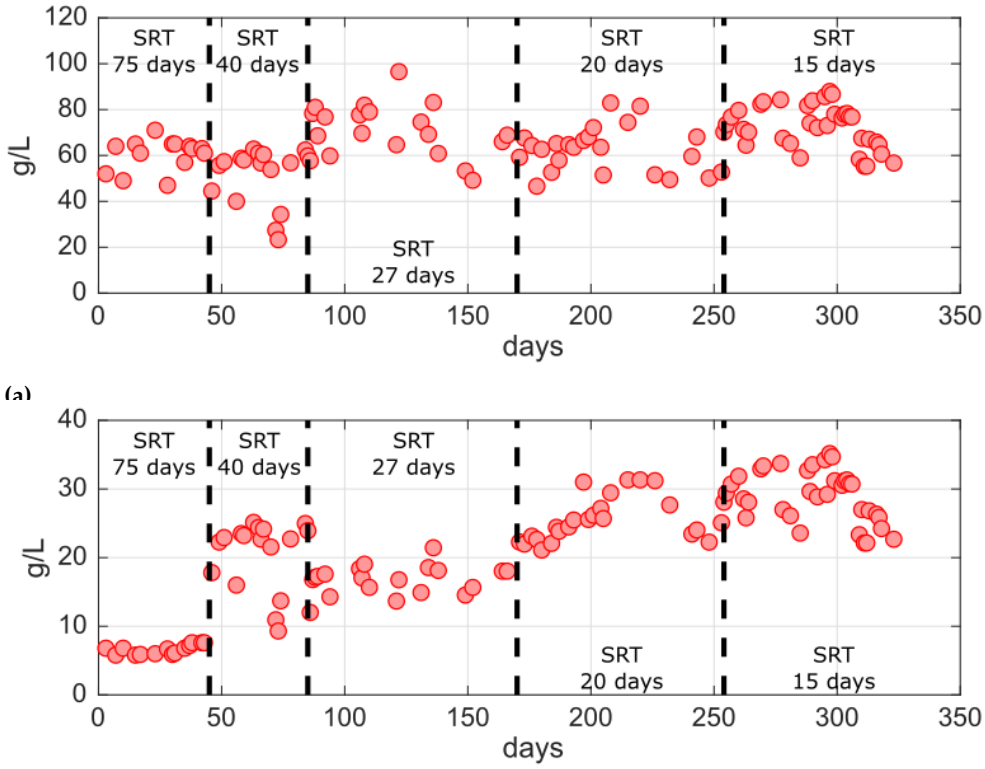

Figure 2. Evolution of the core parameters of the anaerobic digestion process. (**a**) influent concentration of chemical oxygen demand (COD); (**b**) influent concentration of volatile fatty acids (VFA).

In the subsequent stages, over SRT values 27 and 20, the volume of CH_4 remains with no substantial variations over the mean. The volume of CH_4 produced rose moderately once again over the day 210. A moderate stationary tendency is observed beyond the middle of the stage SRT 27 until the day 200. Going beyond data used for modeling purposes, the volume of CH_4 on stage SRT 15 days shows a nonstationary tendency (nonlinear behavior); in some circumstances, the volume of CH_4 produced reached 115 L/day, while in other sections, the volume of CH_4 produced reached almost 20 L/day. The system oscillates

Preprints (www.preprints.org) | NOT PEER-REVIEWED | Posted: 23 August 2022 doi:10.20944/preprints202208.0395.v1

maybe because it was closer to the operational limits.

Figure 4a shown the consequences of the reactor over its operation on pH. From the beginning of stage SRT 40 days until the end of the stage SRT 20, the measurements oscillate around a mean value of 7.7. However, only for informational purposes, although the range SRT 15 days was discarded, it is worth analyzing the high variation in the level of pH due to the reactor producing a high amount of biogas at this stage. Because the system works closely to biochemical and physical limits, the reaction system operates in some cases within unstable regions where production of CH_4 could decrease dramatically due to the well-being of microorganisms and is exposed to uncomfortable scenarios. By the time the value of CH_4 turned chaotic, the value of pH decreases over the limit 7.3 (see Figure stage 15 days).

From the beginning of the data selected, it has been possible to bring about substantial improvement in the volume of CH_4 produced while the values of STR decreased from 40 days to 20 days. However, despite trying to stabilize the variations on the inlet, it was not possible to stabilize the system around a steady state behavior. In the following section, a parameter identification method will be detailed using the data collected from 208 days of measurements.

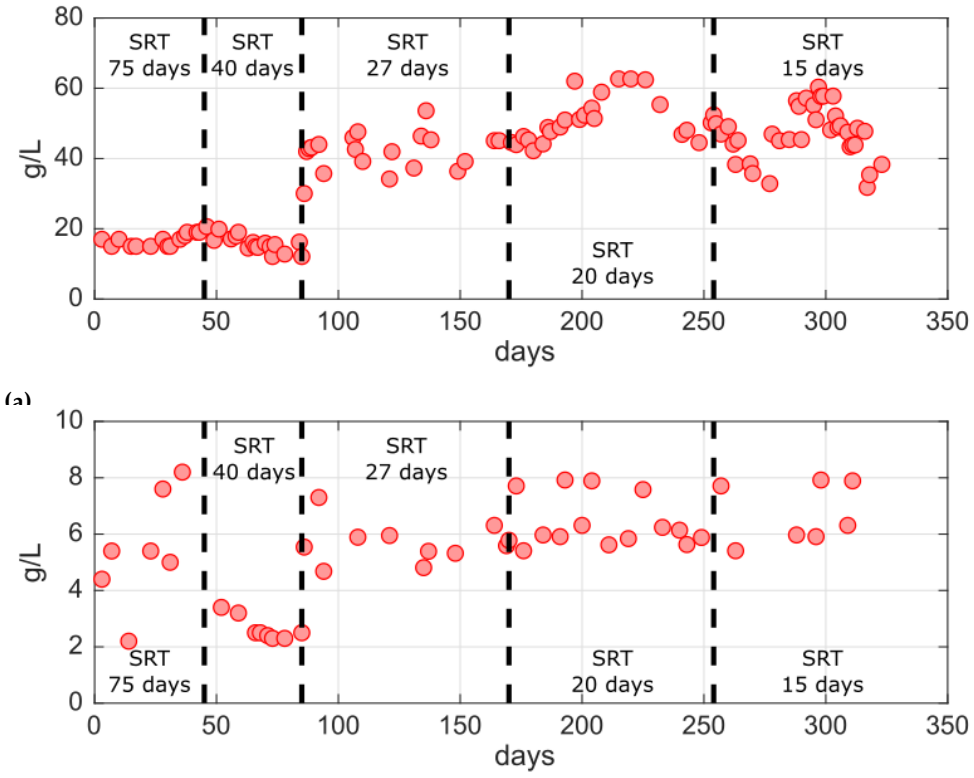

Figure 3. Evolution of the core parameters of the anaerobic digestion process. (**a**) concentration of chemical oxygen demand (COD); (**b**) concentration of volatile fatty acids (VFA).

4. An Adaptive modelling identification strategy for anaerobic digestion reactors

The most common methods used for modeling identification on bioprocess are linear regressions and other strategies based on optimization. The linear regression strategy proposed by Bernard et al. [2] uses the mathematical model ADM2 as the core due it is the best option for control and monitoring purposes. Consequently, the deal is to calculate (calibrate) the set of parameters that assist the mathematical model in closely tracking the experimental data when it runs over the steady-state. The validation procedure is

Preprints (www.preprints.org) | NOT PEER-REVIEWED | Posted: 23 August 2022 doi:10.20944/preprints202208.0395.v1

supported, based on the premise, that the mathematical model has to be evaluated on steady-state and during the process of convergence over transients [4].

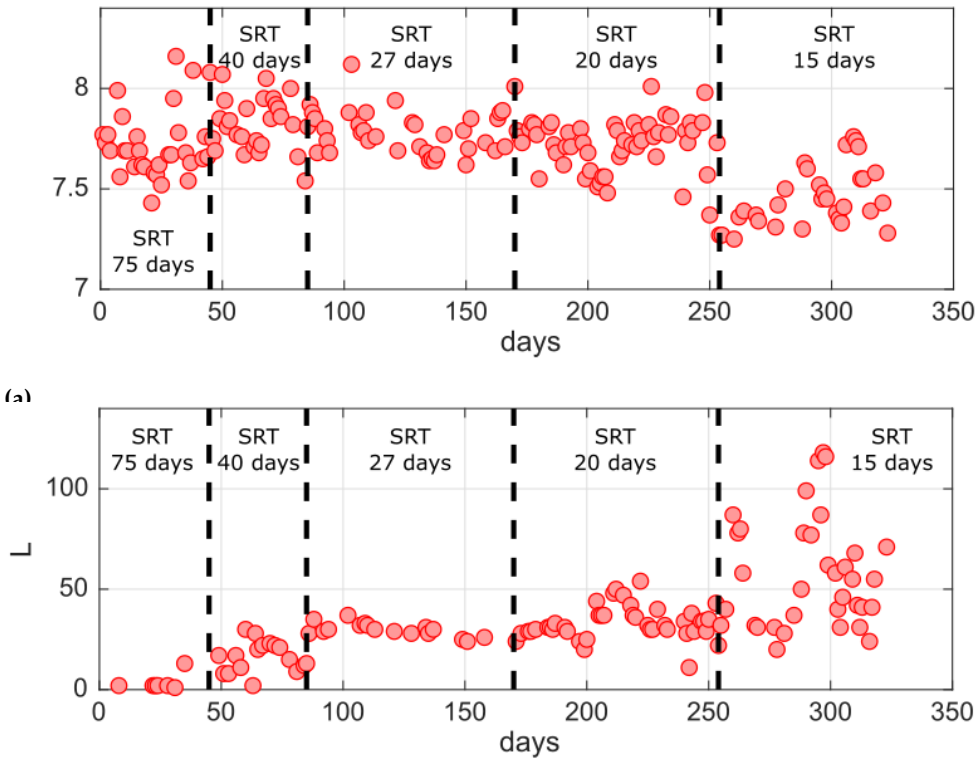

(b)

Figure 4. Evolution of the core parameters of the anaerobic digestion process. (**a**) level of pH; (**b**) methane volume rate production

The transient has been tested step by step once the inlet conditions change. However, despite the numerous advantages; the guarantee of identifiability of parameters, a rigorous identification procedure that covers a wide range of operational conditions, and the ability to validate the performance during transients, especially over unstable phases, the method exhibit disadvantages; the supposition of linearity related with independent and dependent variables, the sensitiveness to noise, the presence of outliers and overfitting [11].

4.1. Parameter identification based on optimization

Consider the mathematical model on equations (1) to (6). The parameters to be identified $p(k)$ are calculated from a parametric identification algorithm that uses the measured information from the reactor, see Figure 5a. The Table 3 below list the parameters to be identified. This method solves an optimization problem to find the values of parameters aiming to minimize the difference between the measured data from the experiment and the same variables considered on the mathematical model ADM2 modified [12]. Figure 5a shows a schematic that explains the architecture proposed. The variables used from the data of the experiment are; $F_{out} = \{CH_4\}$, the volume of methane produced as a consequence of the metabolism by methanogenic archaeas; $n_m = \{S_1, S_2, Z\}$, the measured states considered by the mathematical model ADM2, the organic substrate concentration, volatile fatty acids concentration, and total alkalinity; and finally, the level of pH [13,14].

The variables COD_{in}, VFA_{in}, and D are the chemical oxygen demand, the volatile fatty acids, and the dilution rate, all at the inlet. The input profiles test the system around a wide range of operational scenarios. Q_{in} is the energy used to maintain the reactor within a thermophilic range (not considered by the mathematical model). Figure 5b shown the rules used by the parametric identification algorithm to calculate the optimal parameters $p(k)$.

Preprints (www.preprints.org) | NOT PEER-REVIEWED | Posted: 23 August 2022 doi:10.20944/preprints202208.0395.v1

Table 3. Nomenclature of parameters to be identified on the optimization algorithm.

Parameter	Description	Unit
$\mu_{1_{max}}$	Maximum acidogenic bacteria growth rate	d^{-1}
$\mu_{2_{max}}$	Maximum metanogenic bacteria growth rate	d^{-1}
K_{S_1}	Half saturation constant	g/L
K_{S_2}	Half saturation constant	$mmol/L$
k_1	Yield for substrate degradation	[]
k_2	Yield for VFA production	$mmol/g$
k_3	Yield for VFA consumption	$mmol/g$
k_4	Yield for CO_2 production	$mmol/g$
k_5	Yield for CO_2 production	$mmol/g$
k_6	Yield for CH_4 production	$mmol/g$
K_{Z_1}	Yield for aminoacids degradation	$mmol/L$
K_{Z_2}	Yield for proteins degradation	$mmol/L$
Z_{in}	Total alkalinity at inlet	$mmol/L$

The most important restriction is that the values of parameters have to be the same during the experiment. It allows the mathematical model to evolve ($\hat{x}$), trying to adjust the values of states and other variables to data collected from the experiment (gray line) [15].

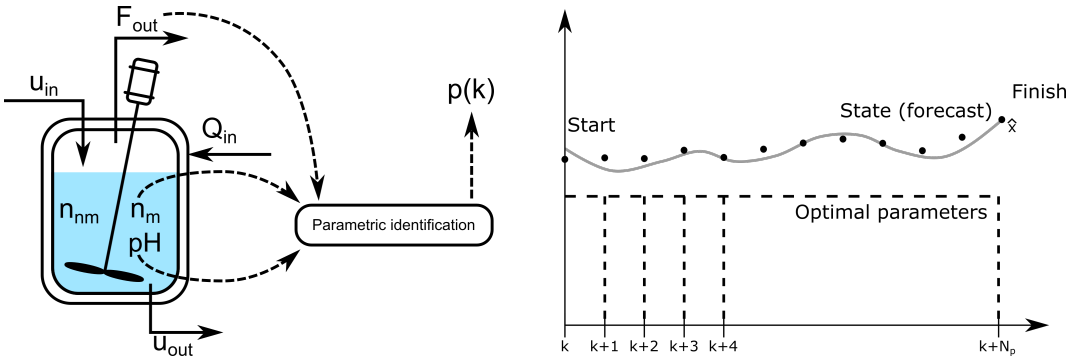

(a) **(b)**

Figure 5. Optimal-based schematics procedures. (**a**) identification parametric diagram; (**b**) identification parametric algorithm.

The following equation (13) shows the optimization problem proposed to be solved.

$$\begin{aligned} &\min_{p(k),\ldots,p(k+N_F)} J(u(k),p(k),x(k)) \\ &\text{s.t.} \\ &\quad x(k+1) = f(x(k),p(k)), \\ &\quad y(k) = g(x(k),u(k)), \\ &\quad y_{min} \leqslant y(k) \leqslant y_{max}, \forall k = 1,\ldots,N_p, \\ &\quad p_{min}, \leqslant u(k) \leqslant p_{max}, \forall k = 1,\ldots,N_u \end{aligned} \tag{13}$$

The equation $J(u(k),p(k),x(k))$ is the functional cost that contains the criteria to minimize. It depends on the parameters $p(k)$ to compute, the output function $y(k)$, and the states variables of the mathematical model $x(k)$. $g(\cdot)$ represents the reference signal introduced. y_{min} and y_{max} are the lower and upper operational constraints. Finally, p_{min} and p_{max} are the lower and upper limits of the parameters to be calculated, hence, $p(k)\ \epsilon\ \{\mu_{1max}, \mu_{2max}, K_{S_1}, K_{S_2}, k_1, k_2, k_3, k_4, k_5, k_6, K_{Z_1}, K_{Z_2}, Z_{in}\}$.

Preprints (www.preprints.org) | NOT PEER-REVIEWED | Posted: 23 August 2022 doi:10.20944/preprints202208.0395.v1

$$J(u(k), p(k), x(k)) = norm\Big((x_{mod}(k) - x_e)^2\Big) \tag{14}$$

The previous equation (14) shows the cost function; the norm of the squared difference between the mathematical model variables and dynamics $x_{mod}(k)$ and the correspondent variables $x_e(k)$ measured on the experimental data. Finally, the following equation shows the variables used in detail.

$$\begin{aligned} J(n_m(k), u(k)) = & norm\Bigg(\Big(n_m^{mod}(k) - n_m^e(k)\Big)^2 + \\ & \Big(pH^{mod}(k) - pH^e(k)\Big)^2 + \Big(q_M^{mod}(k) - q_M^e(k)\Big)^2\Bigg) \end{aligned} \tag{15}$$

The previous equation represents the mean square error between the experimental data ($n_m^e(k)$, $pH^e(k)$ y $q_M^e(k)$) and the correspondent data obtained by the mathematical model ($n_m^{mod}(k)$, $pH^{mod}(k)$ y $q_M^{mod}(k)$). On $n_m(k)^{mod}$ and $n_m(k)^e$ the subscript m represents the dynamics with information over the experiment. The parameters to be computed are $p(k)$.

4.2. On-line identification strategy

Finally, the best alternative is to use a mathematical model that uses both; static parameters influenced by the waste composition and nitrogen content and the online estimation of kinetic parameters due to their large variation. The identifiability of its parameters is conditioned by isolated structures conformed into subsystems that depend on natural interactions. The equations (1) and (3) can be grouped in one subsystem because the state variables S_1 and X_1 are not influenced by others, and so, by the correspondent parameters. Then, the subsystems composed by equations (1), (3) and (2), and (4) can be considered independently. Under normal operation scenarios, the reactor has three equilibrium operational points. The first occurs when the reactor operates under a stable region over operational constraints. The second is when the system operates under instability scenarios, and the third is when the reactor experiment a wash out, so that $X_1 = 0$ and $S_1 = S_{1in}$. When the subsystem composed by the equations (1) and (3) converges, the equations (2) and (4) will do the same towards over an stability region. In the same way, the equations (5) and (6) will converges at the same time [16,17].

4.2.1. Static parameter identification procedure: genetic algorithms

Genetic algorithms evolve inspired by the ability of nature to adapt and evolve conditioned by the environment and the genetic characteristics of their predecessors. The algorithm is based on a random rough search around the solution space area; thus, the convergence depends on the number of iterations until the optimal solution is encountered. This option is used as a reference in order to quantify the improvements achieved on the algorithm proposed in the next section.

4.2.2. Static parameter identification procedure: step ahead

Figure 6a shows the algorithm's structure and the step-by-step designing process to estimate the static parameters over the process. The technique, called step-ahead, place a mathematical model as the core to predict the evolution of the system dynamics over each time step determined. Consider X_0 as the starting point (represented by a black circle •). At this time, the algorithm uses the mathematical model to calculate the next step forward, aiming to discover the system's evolution in advance (represented by a black triangle ▲). Now, on X_1, the new measured value (the •) is compared with prediction (the ▲). The difference between the values of • and ▲ (• − ▲) means the error aiming to minimize over the experiment. To calculate the prediction of the system in advance, in X_0 is required the information of; the initial conditions, the inputs u_s, and the value of the parameters to be calculated p.

Preprints (www.preprints.org) | NOT PEER-REVIEWED | Posted: 23 August 2022 doi:10.20944/preprints202208.0395.v1

$$E = [error_1, error_2, ..., error_n] \tag{16}$$

In the next step, aiming to perform a new prediction (on X_1), the algorithm updates the initial conditions (replacing the value of the previous prediction ▲ with the new initial condition, or measurable value, ●). This strategy allows adjusting the deviation (or error) on each step. The end of the simulation results in a vector that stores all the errors encountered over each step [18].

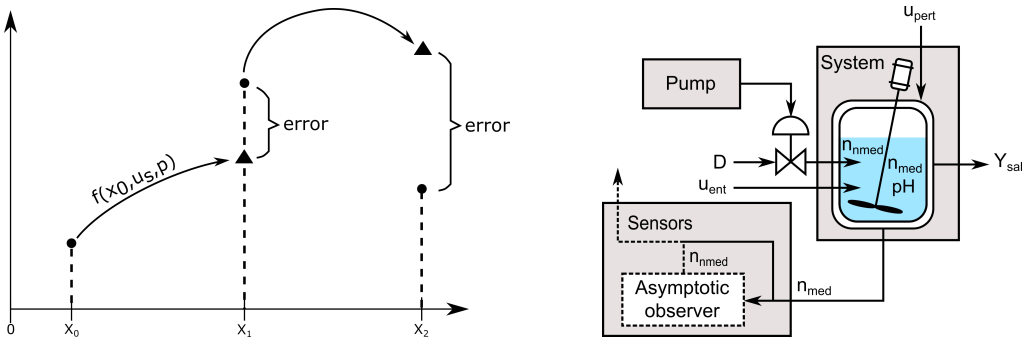

(a) **(b)**

Figure 6. The proposed structures in the anaerobic digestion process. (**a**) step-ahead algorithm; (**b**) asymptotic observer structure.

The objective of the optimization problem to be solved changes; however, the restrictions and operational boundaries are the same compared with equations 13. The new optimization problem is shown in the following equations.

$$\min_{u(k)} E \tag{17}$$

s.t.

$$\begin{aligned} & n_m(k+1) = f(n_m(k), u(k)), \\ & n_{nm}(k+1) = f(n_{nm}(k), u(k)), \\ & 0 \leqslant u(k) \leqslant p_{max}, \forall k = 1, ..., t_f \end{aligned} \tag{18}$$

4.2.3. Dynamic parameters: an asymptotic observer in anaerobic digestion processes

One significant problem with using control and monitoring systems in anaerobic digestion reactors; it is not yet possible to achieve all measurements online to feed the mathematical model and start operations with a controller. However, the absence of information due to the lack of reliable sensors, and the inadequate strategies to test constantly all measurements made by laboratory analyses, opens up an opportunity to substitute the uncertainty by using online software sensors.

The online software sensors, or the so-called state observers (in control and engineering theory), estimate the state variables inside the homogeneous reaction systems using other measurements tied to the given system. Based on the previously existing information (the reaction kinetics and the static parameters), different state observers are proposed in the literature. The data from reaction kinetics is unknown; therefore, this observer is a consequence of the strictly challenging requirement that the information from kinetics needs to be known. This results in a particular category of observers named asymptotically because it estimates the non-existing measurable states based on two conditions; the system is still not exponentially observable, and the reaction kinetics are unknown. The design of the algorithm has to fulfill the following conditions: the information of matrix ϕ is

Preprints (www.preprints.org) | NOT PEER-REVIEWED | Posted: 23 August 2022 doi:10.20944/preprints202208.0395.v1

unknown, the yield coefficients from K are fully known, and finally, the number of q_{state}, the number of measured state variables is the same or higher than the rank of the matrix K, that is $q_{state} = dim(\xi_1) \geq= rank(K)$. First, consider the general homogeneous reaction systems described by the general nonlinear state space model, that is.

$$\frac{d\xi}{dt} = K\phi(\xi, t) - D\xi - Q(\xi) + F. \tag{19}$$

Where $dim(\xi) = dim(F) = dim(Q) = N$, $dim(\phi) = M$ and $dim(K) = N \times M$. The general nonlinear model equation (19) can be divided as.

$$\frac{d\xi_a}{dt} = K_a\phi(\xi_a, \xi_b) - D\xi_a - Q_a + F_a, \tag{20}$$
$$\frac{d\xi_b}{dt} = K_b\phi(\xi_a, \xi_b) - D\xi_b - Q_b + F_b, \tag{21}$$

Where the rank of K is p. The submatrix K_a comes from K and the dimensions are $p \times M$. The submatrix K_b has the remaining information of K. Finally, the matrices (ξ_a, ξ_b), (Q_a, Q_b) and (F_a, F_b) are the corresponding parts of ξ, Q and F caused by the influence of K_a and K_b. The previous formulation has the following feature. There exists a transformation that considers Z_{ob} as a linear combination of X_a and X_b, thus.

$$Z_{ob} = A_0\xi_a + \xi_b. \tag{22}$$

derived from the previous equation.

$$\dot{Z_{ob}} = A_0\dot{\xi}_a + \dot{\xi}_b. \tag{23}$$

then, using the equation (20) on the equation (23):

$$\dot{Z_{ob}} = A_0(K_a\phi - DX_a - Q_a + F_a) + K_b\phi - DX_b - Q_b + F_b. \tag{24}$$

solving the last equation.

$$\dot{Z_{ob}} = A_0K_a\phi - A_0DX_a - A_0Q_a + A_0F_a + K_b\phi - DX_b - Q_b + F_b, \tag{25}$$

then grouping the expressions.

$$\dot{Z_{ob}} = -D(A_0X_a + X_b) + A_0(F_a - Q_a) + F_b - Q_b + A_0K_a\phi + K_b\phi. \tag{26}$$

finally, using the equation (23) on equation (26), then:

$$\dot{Z_{ob}} = -DZ_{ob} + A_0(F_a - Q_a) + F_b - Q_b + \underbrace{\phi(A_0K_a + K_b)}_{eliminate}. \tag{27}$$

there are two conditions in order to remove the expression in (27). However $\phi \neq 0$, thus.

$$A_0K_a + K_b = 0, \tag{28}$$

Finally, according to the previous equations, the state space model is equivalent to.

$$\frac{d\xi_a}{dt} = K_a\phi(\xi_a, \xi_b) - D\xi_a - Q_a + F_a, \tag{29}$$
$$\frac{dZ_{ob}}{dt} = -DZ_{ob} + A_0(F_a - Q_a) + (F_b - Q_b). \tag{30}$$

If the expression $F_a - Q_a = 0$, then it means that the partition made by the equations (20) and (21) are appropriate due to the new dynamics on Z_{ob} are independent from K and ϕ.

Preprints (www.preprints.org) | NOT PEER-REVIEWED | Posted: 23 August 2022 doi:10.20944/preprints202208.0395.v1

Equation (29) shown the values of $\dot{\xi}_a$ independent from ϕ (the information of the reaction kinetics).

Observer design

Using the nonlinear general dynamical model, equations (1) to (6), the following equations describes a decoupled subsystem conducted by the state variables X_1, X_2, S_1 y S_2 that can be run separately. This representation allows working with a reduced model re-written as.

$$\xi = \begin{bmatrix} X_1 \\ X_2 \\ S_1 \\ S_2 \end{bmatrix}, \; F = \begin{bmatrix} 0 \\ 0 \\ DS_{1in} \\ DS_{2in} \end{bmatrix}, \; Q = \begin{bmatrix} 0 \\ 0 \\ 0 \\ 0 \end{bmatrix}, \; K = \begin{bmatrix} 1 & 0 \\ 0 & 1 \\ -k_1 & 0 \\ k_2 & -K_3 \end{bmatrix}, \; \phi = \begin{bmatrix} \mu_1 X_1 \\ \mu_2 X_2 \end{bmatrix}. \tag{31}$$

Considering the previous subsystem, the subsequent state equations are structured as follows.

$$\frac{d}{dt}\begin{bmatrix} X_1 \\ X_2 \\ S_1 \\ S_2 \end{bmatrix} = \begin{bmatrix} 1 & 0 \\ 0 & 1 \\ -k_1 & 0 \\ k_2 & -K_3 \end{bmatrix}\begin{bmatrix} \phi_1 \\ \phi_2 \end{bmatrix} - D\begin{bmatrix} X_1 \\ X_2 \\ S_1 \\ S_2 \end{bmatrix} + \begin{bmatrix} 0 \\ 0 \\ DS_{1in} \\ DS_{2in} \end{bmatrix}. \tag{32}$$

Then, comparing the previous subsystem with the equivalent generic equations (29) and (30) results in the following specifications.

- The original nonlinear state space system was decoupled into two parts; the subsystem equation in (32), and the other part that includes the remaining state variables, inorganic carbon C and total alkalinity Z.
- The information, usually contained on matrices Q_a and Q_b, is located in the state dynamic variable C.
- The matrices Q_1 and Q_2 are the reaction rates r_1 and r_2.

Based on the previous requisites, ξ_a and ξ_b represents the information of measurable and no measurable states, thus.

$$\xi_a = \begin{bmatrix} S_1 \\ S_2 \end{bmatrix}, \quad \xi_b = \begin{bmatrix} X_1 \\ X_2 \end{bmatrix} \tag{33}$$

therefore.

$$Z_{ob} = \begin{bmatrix} Z_{ob_1} \\ Z_{ob_2} \end{bmatrix} = \left[A_0\xi_a + \xi_b\right] = \begin{bmatrix} \frac{1}{K_1} & 0 \\ \frac{K_2}{K_1 K_3} & \frac{1}{K_3} \end{bmatrix}\begin{bmatrix} S_1 \\ S_2 \end{bmatrix} + \begin{bmatrix} X_1 \\ X_2 \end{bmatrix} \tag{34}$$

using $Z = A_1\xi_1 + A_2\xi_2$ to compare with the previous structure in equation (34) results in.

$$A_2 = I \tag{35}$$

as a consequence, in order to find A_0.

$$A_0 = -K_b K_a^{-1} \tag{36}$$

Using the equation (36) and employing the previous information originates the following matrices.

$$K_b = \begin{bmatrix} 1 & 0 \\ 0 & 1 \end{bmatrix}, \; K_a = \begin{bmatrix} -K_1 & 0 \\ K_2 & -K_3 \end{bmatrix}. \tag{37}$$

The next step is to separate the non-measurable states in order to estimate the variables Z_{ob_1} and Z_{ob_2}, and the measurable states S_1 and S_2. Using the equation (22) and solving for ξ_b.

Preprints (www.preprints.org) | NOT PEER-REVIEWED | Posted: 23 August 2022 doi:10.20944/preprints202208.0395.v1

$$\xi_b = Z_{ob} - A_0\xi_a \tag{38}$$

At this point we have the matrices of ξ_a, A_0 and Z_{ob}.

$$\xi_b = \begin{bmatrix} X_1 \\ X_2 \end{bmatrix}, \quad Z_{ob} = \begin{bmatrix} Z_{ob_1} \\ Z_{ob_2} \end{bmatrix}, \quad A_0 = \begin{bmatrix} \frac{1}{k_1} & 0 \\ \frac{k_2}{k_1 k_3} & \frac{1}{k_3} \end{bmatrix}, \quad \xi_b = \begin{bmatrix} S_1 \\ S_2 \end{bmatrix} \tag{39}$$

The state variables X_1 and X_2 are unknown. The variables Z_{ob_1} and Z_{ob_2} represent the new dynamics independent from the reaction kinetics contained on ϕ. The matrix A_0 has the yield coefficients, and the state variables S_1 and S_2 are the estimation space. The values of F_a and F_b are.

$$F_a = \begin{bmatrix} DS_{1in} \\ DS_{2in} \end{bmatrix}, \quad F_b = \begin{bmatrix} 0 \\ 0 \end{bmatrix} \tag{40}$$

Finally, with the use of the previous equations, the expression of Z_{ob} is as follows [19].

$$\frac{dZ_{ob}}{dt} = -DZ_{ob} + A_0(Fa - Q_a) + (F_b - Q_b) \tag{41}$$

5. Results

Figure 7 shown the data used to feed the reactor during the experiment, the inputs considered are $S_{1_{in}}$, $S_{2_{in}}$, Z_{in} and D. Figure 7c shown the value of $S_{1_{in}}$.

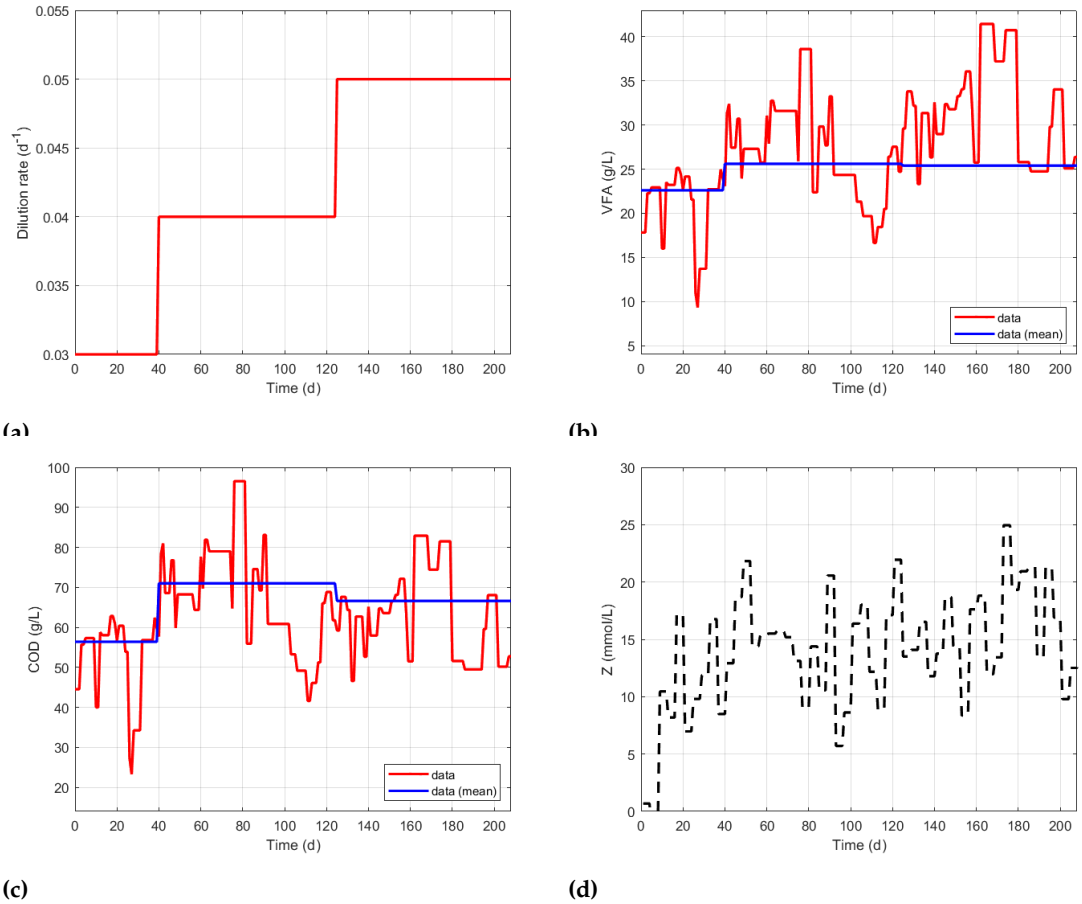

Figure 7. Influent measurements on anaerobic digestion process. (**a**) dilution rate (D); (**b**) volatile fatty acids (VFA); (**c**) chemical oxigen demand (COD); (**d**) alkalinity (Z).

The red line represents the value measured of COD on influent. However, for simulation purposes, it is considered a constant value over the three stages (the same changes that

Preprints (www.preprints.org) | NOT PEER-REVIEWED | Posted: 23 August 2022 doi:10.20944/preprints202208.0395.v1

occur on the value D) represented by the blue line. The same procedure was proposed to the value $S_{2_{in}}$ (VFA). Finally, on Figure (7d), the optimizer calculates the data to reconstruct Z_{in}. This variable was computed along the experiment because the total alkalinity Z at the inlet was not measured by M.A. de la Rubia [10]. The condition inserted on the optimization algorithm is that Z_{in} maintain its value constant over four days, trying to replicate the measurements made on-site.

Figure 8 shows the results achieved by the parametric identification algorithm using experimental data. Figures 8a and 8b present the adjustment achieved by the state variables S_1 and S_2 between the mathematical model and the experimental data, the chemical oxygen demand and volatile fatty acids respectively. The red line represents the actual data measured from the experiment, and the blue line (only for informative purposes) is the mean value used as a reference where the system theoretically be established on steady-state (due to the dilution rate D remains constant). The discontinuous black line is the dynamic of the mathematical model that better adjusts to the experimental data.

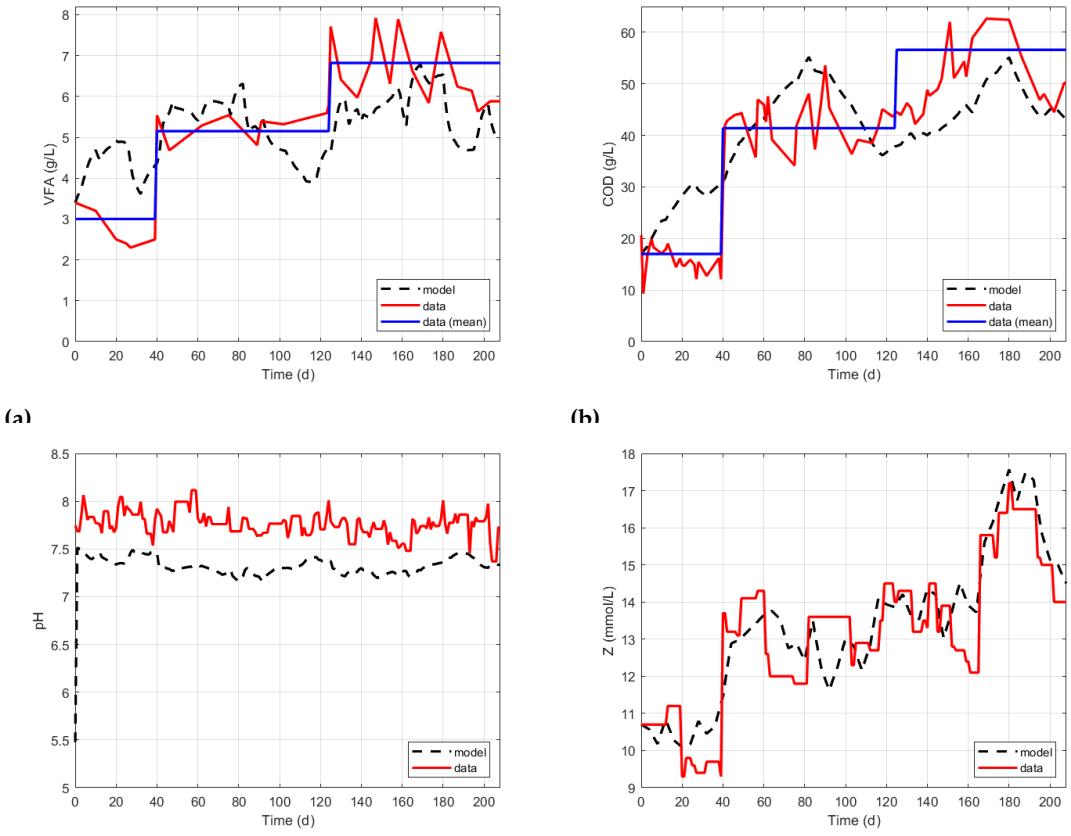

Figure 8. The use of genetic algorithms to fit the mathematical model to the experimental data. (**a**) volatile fatty acids (VFA); (**b**) chemical oxigen demand (COD); (**c**) level of pH; (**d**) alkalinity (Z).

The pH value achieves desirable results because the difference between the experimental data and the mathematical model is relatively close. Only at the beginning was the difference very high due to the initial conditions set on the simulator. Finally, Figure 8d shows the results of the identification procedure made for total alkalinity Z. The dynamic of the mathematical model (discontinuous black line) closely follows the reference (the measured data, the red line).

Figure 9a shows the results after running the parameter identification genetic algorithm conditioned trajectory volume of methane CH_4 produced. The discontinuous black line

Preprints (www.preprints.org) | NOT PEER-REVIEWED | Posted: 23 August 2022 doi:10.20944/preprints202208.0395.v1

that represents the mathematical model adjusted to the data by the parameters follows the variations closely.

Figure 10a and Figure 10b shown the improvement achieved by the use of the step-ahead algorithm. For the dynamics S_1 and S_2, the difference between the discontinuous black line (mathematical model) and the experimental data (red line) is closer than the previous results. Figure 10c shows the results of the new algorithm with the pH value. As it is being shown, there is a significant improvement compared with the previous results.

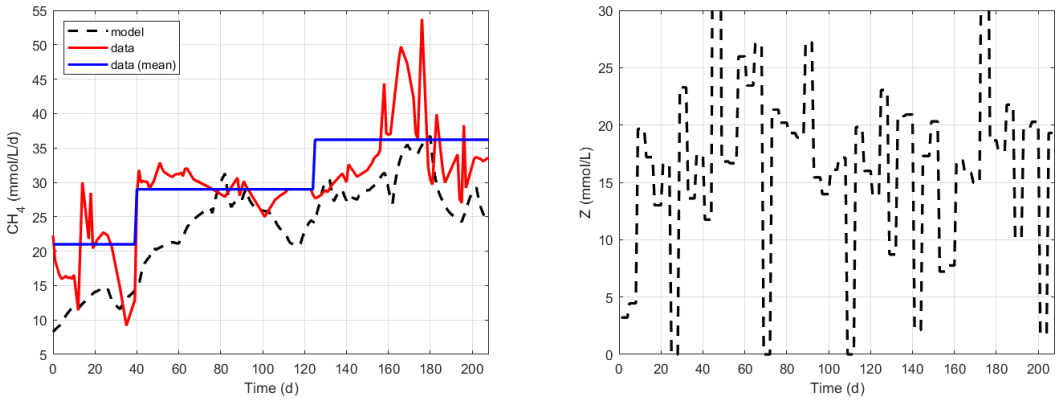

(a) **(b)**

Figure 9. The use of genetic algorithms to fit the mathematical model to the experimental data. (**a**) the volume of methane (CH_4). (**b**) Influent alkalinity results using the algorithm step-ahead.

Figure 10d shows the results of the adjustment achieved by the total alkalinity using the algorithm step-ahead. There is a significant improvement compared with the previous results (see Figure 10d). Figure 11a shows the results between the mathematical model (discontinuous black line) and the experimental data (red line) achieved in the volume of methane CH_4 produced [10,20].

Table 4. Values of parameters achieved by the two algorithms; genetic algorithm (GA) and step ahead (SA)

Parameter	Value		Unit
	GA	SA	
$\mu_{1_{max}}$	0.26	0.06	d^{-1}
$\mu_{2_{max}}$	1.52	0.05	d^{-1}
K_{S_1}	213.89	298.03	g/L
K_{S_2}	168.76	1.08	$mmol/L$
k_1	29.34	$1.34x10^{-6}$	[]
k_2	31.14	216.80	$mmol/g$
k_3	40.81	14.23	$mmol/g$
k_4	36.61	$8.58x10^{-7}$	$mmol/g$
k_5	43.21	$1.14x10^{-6}$	$mmol/g$
k_6	549.99	550.00	$mmol/g$
K_{Z_1}	0.68	3.21	$mmol/L$
K_{Z_2}	1.28	4.45	$mmol/L$
Z_{in}	$V_{Z_{in}}$	19.66	$mmol/L$

Finally, based on previous results, to quantify the improvement achieved by the new algorithm, Figure 11b is focused on measuring the improvements in the variables VFA, COD, Z, pH and CH_4. The performance achieved by the genetic algorithm is used as a reference (see the results in Table 5). The equation used to calculate the performance is (42). Table 6 shown the values calculated by solvers.

Preprints (www.preprints.org) | NOT PEER-REVIEWED | Posted: 23 August 2022 doi:10.20944/preprints202208.0395.v1

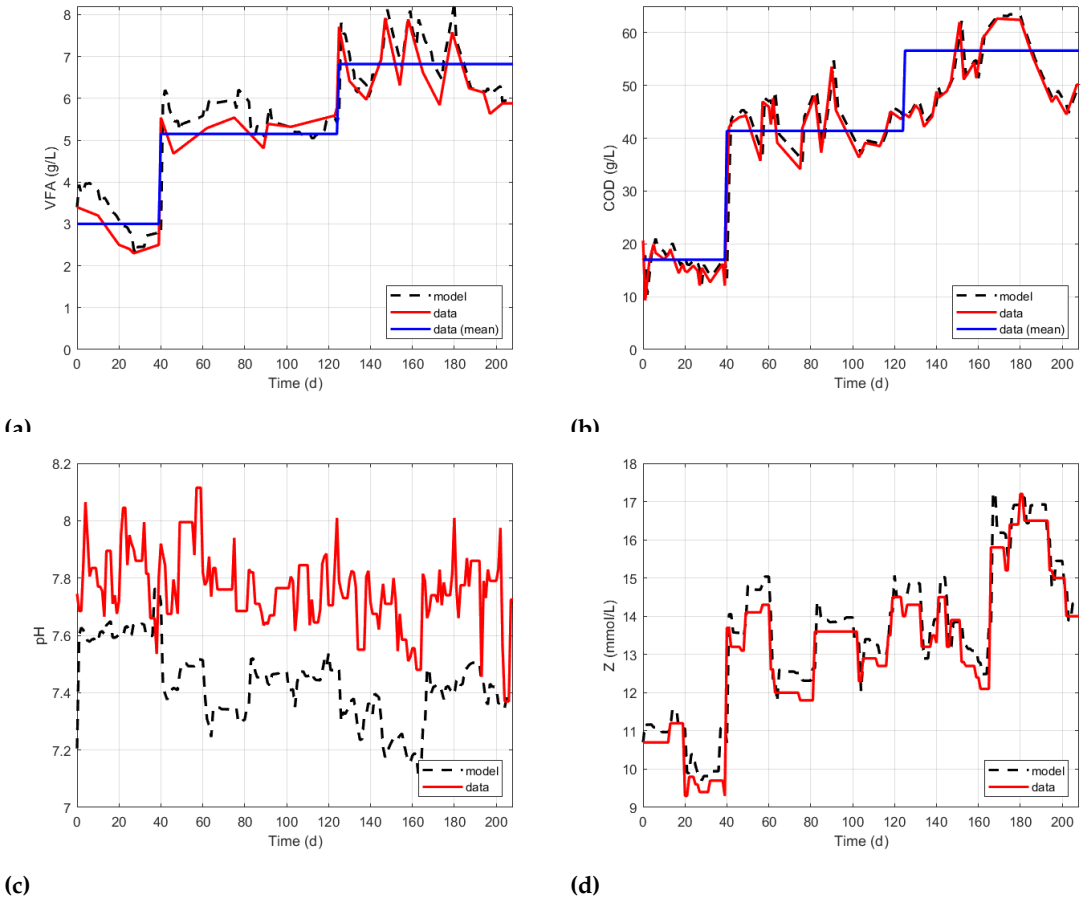

Figure 10. Step-ahead algorithms to fit the mathematical model to the experimental data. (**a**) volatile fatty acids (VFA); (**b**) chemical oxygen demand (COD); (**c**) level of pH; (**d**) alkalinity (Z).

Finally, after 60 days, both dynamics converge. Once the dynamics of the mathematical model and the estimator run together, both react instantly simultaneously due to changes. On day 50, a change in the operational point occurred; the value of the dilution rate changed from 0.03 to 0.07.

$$\% \text{ Improvement} = 100 - \frac{100 \sum_{k=1}^{208} S_1(k)^{sa} - S_1(k)^{exp}}{\sum_{k=1}^{208} S_1(k)^{ga} - S_1(k)^{exp}} \tag{42}$$

As shown in Figure 12, both concentration of acidogenic and methanogenic bacterias drastically reduce their presence in the reactor. Even when the dynamics were about to achieve a stabilization point, a new change on day 100 was carried out; the dilution rate changed from 0.07 to 0.05. Both the dynamics of the mathematical model and the estimation algorithm continue running together towards its natural behavior.

Table 5. Evaluation of the adjustment achieved by the parameter identification strategies; genetic algorithm and step-ahead.

Variable	S_1	S_2	Z	pH	CH_4
% Improvement	78.7	60.5	38.6	25.5	7.7

Preprints (www.preprints.org) | NOT PEER-REVIEWED | Posted: 23 August 2022 doi:10.20944/preprints202208.0395.v1

From that moment, the dynamics of the mathematical model and the observer remained together.

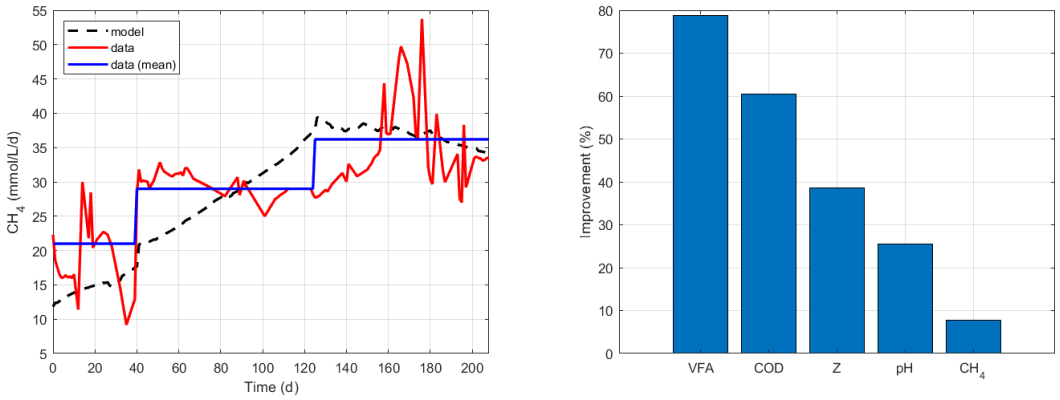

(a) **(b)**

Figure 11. Step-ahead algorithm used to adjust the mathematical model to experimental data. (**a**) the volume of methane (CH_4). (**b**) Fitting improvement from step-ahead compared with genetic algorithm.

All aforementioned demonstrates that the asymptotic observer has good performance.

Table 6. Values of the parameters selected.

Parameter	Value		Unit
	GA	SA	
$\mu_{1_{max}}$	0.26	0.06	d^{-1}
$\mu_{2_{max}}$	1.52	0.05	d^{-1}
K_{S_1}	213.89	298.03	g/L
K_{S_2}	168.76	1.08	$mmol/L$
k_1	29.34	$1.34x10^{-6}$	[]
k_2	31.14	216.80	$mmol/g$
k_3	40.81	14.23	$mmol/g$
k_4	36.61	$8.58x10^{-7}$	$mmol/g$
k_5	43.21	$1.14x10^{-6}$	$mmol/g$
k_6	549.99	550.00	$mmol/g$
K_{Z_1}	0.68	3.21	$mmol/L$
K_{Z_2}	1.28	4.45	$mmol/L$
Z_{in}	$V_{Z_{in}}$	19.66	$mmol/L$

Then, Figure 6b shows the structure proposed by direct measurement (Sensors) and the asymptotic observer that estimates the state variables X_1 and X_2. This structure seeks to address the lack of measurements due to the absence of reliable sensors. Figure 12 shows the results obtained by the algorithm asymptotic observer that reconstruct the state variables concentration of acidogenic X_1 and methanogenic X_2 bacterias. To test the observer's performance, the values of estimations were compared with the dynamics measured directly from the mathematical model. The starting point between the simulation of the dynamic observer and the mathematical model was different in order to confirm the convergence between them sometime.

Preprints (www.preprints.org) | NOT PEER-REVIEWED | Posted: 23 August 2022 doi:10.20944/preprints202208.0395.v1

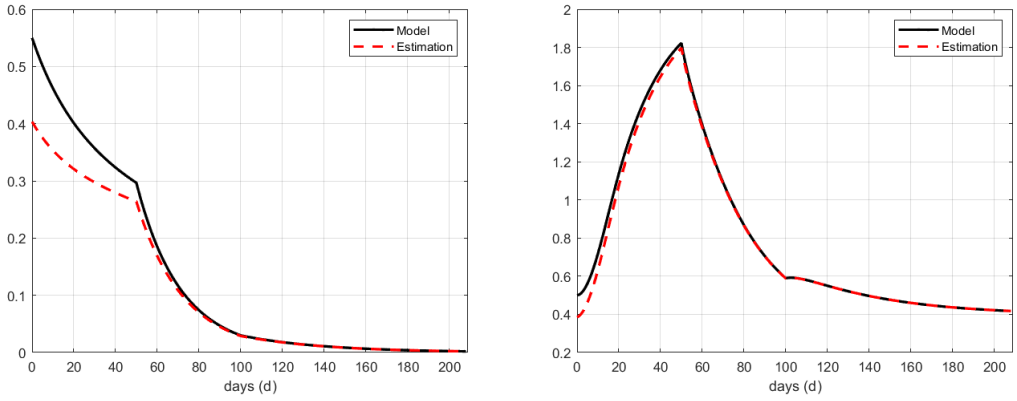

(a) **(b)**

Figure 12. Performance test for the asymptotic observer. (**a**) model variable X_1; (**b**) model variable X_2.

6. Conclusions

This paper proposes a structure composed of an asymptotic observer and a parameter identification procedure based on optimization, aiming to measure continuous online data to feed the mathematical model and run algorithms for control and monitoring purposes. The proposed structure replaces traditional actions in the industry where the lack of information is replaced by generic values found in the literature (rates of microorganisms like substrate degradation fairly the same chemical and operational conditions). The module's operation starts with the parameter identification algorithm that, based on its optimization programming, finds the value of the best parameters that better minimize the difference between the data measured and the dynamics of the mathematical model by tunning the variables (degrees of freedom). The step-ahead algorithm, based on optimization, was tested with success; the performance was compared with a traditional optimization method (genetic algorithm). Using as a reference, the results obtained by the genetic algorithm were compared with those obtained by the step-ahead algorithm. The improvement was calculated using five variables; S_1, S_2, Z, pH and $CH4$. The results shown improvements from 7.7 % for 78.7 % in CH_4 to achieved by S_1. Once the parameters were calculated Additionally, the absence of online measurements from the concentration of microorganisms (acidogens and methanogens) gives affordable times for control purposes; it was necessary to choose an asymptotic observer strategy to have the chance to approximate these measurements in advance instead of having data from traditional methods but with extended dwell times. New variables were added to the mathematical model ADM2 (inspired by other modifications found in the literature on this model) to extend the set of usable types of organic matter. The methodology mentioned above aims to enable this algorithm as the basis for designing a wide range of possibilities of control structures forward.

1. Front Matter. In *On-line Estimation and Adaptive Control of Bioreactors*; Bastin, G.; Dochain, D., Eds.; Process Measurement and Control, Elsevier: Amsterdam, 1990.
2. O., B.; Z., H.S.; D., D.; A., G.; J.P., S. Dynamical model development and parameter identification for an anaerobic wastewater treatment process. *Biotechnol Bioeng* **2001**, *75*, 424–438.
3. Batstone, D.; Keller, J.; Newell, B.; Newland, M. Model development and full scale validation for anaerobic treatment of protein and fat based wastewater. *Water Science and Technology* **1997**, *36*, 423–431. doi:10.2166/wst.1997.0619.
4. Batstone, D.; Keller, J.; Angelidaki, I.; Kalyuzhnyi, S.; Pavlostathis, S.; Rozzi, A.; Sanders, W.; Siegrist, H.; Vavilin, V. Anaerobic digestion model No 1 (ADM1). *Water science and technology : a journal of the International Association on Water Pollution Research* **2002**, *45*, 65–73.
5. Hoil, K.; Li, D.; Yugeng, X.; Jiwei, L. Model predictive control with on-line model identification for anaerobic digestion processes. *Biochemical Engineering Journal* **2017**, *128*, 63–75.

6. Monteiro, E.; Ferreira, S. Biomass Waste for Energy Production. *Energies* **2022**, *15*. doi:10.3390/en15165943.
7. Rossi, E.; Pecorini, I.; Ferrara, G.; Iannelli, R. Dry Anaerobic Digestion of the Organic Fraction of Municipal Solid Waste: Biogas Production Optimization by Reducing Ammonia Inhibition. *Energies* **2022**, *15*. doi:10.3390/en15155515.
8. Andrews, J.F. A mathematical model for the continuous culture of microorganisms utilizing inhibitory substrates. *Biotechnology and Bioengineering* **1968**, *10*, 707–723.
9. Song, Y.J.; Oh, K.S.; Lee, B.; Pak, D.W.; Cha, J.H.; Park, J.G. Characteristics of Biogas Production from Organic Wastes Mixed at Optimal Ratios in an Anaerobic Co-Digestion Reactor. *Energies* **2021**, *14*. doi:10.3390/en14206812.
10. de la Rubia, M.; Perez, M.; Romero, L.; Sales, D. Effect of solids retention time (SRT) on pilot scale anaerobic thermophilic sludge digestion. *Process Biochemistry* **2006**, *41*, 79–86.
11. Marquez-Ruiz, A.; Mendez-Blanco, C.; Ozcan, L. Constrained Control and Estimation of Homogeneous Reaction Systems Using Extent-Based Linear Parameter Varying Models. *Industrial Engineering Chemistry Research* **2020**.
12. Marquez-Ruiz, A.; Mendez-Blanco, C.; Porru, M.; Özkan, L. State and Parameter Estimation Based On Extent Transformations. *Computer Aided Chemical Engineering* **2018**, *44*, 583–588.
13. R., C.; H., T.; T., H. Hydrotermal pretreatment of rice straw biomass: A potential and promising method for enhanced methane production. *Appl. Energy* **2012**, *94*, 129 – 140.
14. Hanema, J.; Lazar, M.; Tóth, R. Tube-based LPV constant output reference tracking MPC with error bound. *IFAC-PapersOnLine* **2017**, *50*, 8612–8617.
15. Hassam, S.; Ficara, E.; Leva, A.; Harmand, J. A generic and systematic procedure to derive a simplified model from the anaerobic digestion model No. 1 (ADM1). *Biochemical Engineering Journal* **2015**, *99*, 193–203.
16. Haldane, J. Enzynmes. *MIT Press* **1965**, p. 184.
17. Isaza-Hurtado, J.; Botero-Castro, H.; Alvarez, H. Robust estimation for LPV systems in the presence of non-uniform measurements. *Automatica* **2020**, *115*, 108901.
18. B., S.; M., A.; D., B. American Institute of Chemical Engineers. *AIChE Journal* **1998**, *44*, 1858–1867.
19. Costello, D.; Greenfield, P.; Lee, P. Dynamic modelling of a single-stage high-rate anaerobic reactor—I. Model derivation. *Water Research* **1991**, *25*, 847–858.
20. López Buriticá, K.; Trujillo, S.; Acosta-Medina, C.; Granada D., H. Dynamical Analysis of a Continuous Stirred-Tank Reactor with the Formation of Biofilms for Wastewater Treatment. *Mathematical Problems in Engineering* **2015**, *2015*.